(Preprint) AAS 19-379

EFFECTS OF SPIN-ORBIT RESONANCE IN STABILITY FOR LOW ALTITUDE MARS ORBITS

Andres Dono and Laura Plice

Orbit stability has been thoughtfully studied in various celestial bodies. The increasing interest in Mars orbiters brings the question of the likelihood of natural decay in low altitude regimes. This paper studies the shape change of low altitude Mars orbits by carrying out large sets of numerical high fidelity simulations. Results showed that various configurations of the orbital elements gave perturbations that resulted in unstable orbits. The paper also studies the potential causes of the observed unstable regions. We computed theoretical spin-orbit resonances to study their implications in the stability at low altitudes. The resonances were tested at different initial Longitudes of the Ascending Node (LAN) and orbit inclinations to check the potential existence of latitude/longitude implications on the stability.

INTRODUCTION

Orbit stability represents a major concern for spacecraft mission design. Spacecraft orbiting at low altitude are subject to the effects of irregular gravity fields and atmospheric drag. Therefore, it is important to address this issue for potential upcoming missions, especially in celestial bodies other than Earth that may not be as well characterized since the number of orbiting missions is smaller. The Moon is one of the celestial bodies that has attracted most interest over recent years due to its chaotic stability environment at low altitudes, caused by uneven distributions or mass concentrations, or mascons[1] from now on. The lunar PFS-2 orbiter was one of the first man-made objects influenced by the effects of non-uniform gravity. During the early stages of the mission, the lumpiness of the lunar gravity field severely reshaped the initial orbit of the satellite and led to a collision in as short as 35 days after its insertion. Since then, many studies, simulations, and theories about lunar orbit stability have been carried out in the literature. Previous work by Folta and Quinn (2006)[2] performed several orbit propagations to study the evolution of the argument of periapsis and eccentricity in polar plots over time, while Plice et al. studied the evolution of these elements by using contour plots and heat maps[3]. Some of these publications successfully identified stable regions where the shape of the orbit was not altered sensibly over long periods of time.

For other objects in the Solar System, previous work addressed the needs of past spacecraft mission designs, however, the amount of research done for other planets is not comparable to the number of publications that study the stability in lunar orbits. The orbit stability research at Mars is not as extensive as in the case of the Moon. Some papers by Alvarellos[4]and Silva[5] studied the effects of the mascons in aerostationary orbits, identifying key longitudes where the satellites remain more robust to the perturbations. However, there are not many publications addressing the

stability at low Martian orbit altitudes. We can leverage the lunar orbit stability research to apply similar techniques and studies to the case of Mars.

Frozen orbits are one of the main research topics regarding stability around a celestial body. These characteristic orbits maintain a quasi-stable configuration of the orbital elements. In particular, eccentricity, semi-major axis (sma), and argument of periapsis present little or no secular changes. An extensive effort in the analysis of lunar orbits was carried by Meyer et al., 1994[6]. This publication proposed suitable methods for preliminary design level for lunar mission planning. It included a detailed description of mascons and spherical harmonics models, to compute lifetime and stability analysis. More than a decade later, a detailed mathematical analysis of the dynamics for low altitude orbits was developed to find critical inclinations at which frozen orbital element configurations are obtained (Abad et al., 2009)[7]. Lara et al., also (2011)[8] placed the focus in the analytical implications of the irregularities of the lunar gravity field. In parallel, Ely et al.[9], found that low inclination orbits have an extreme variability in their evolution, while for nearly polar inclinations, there are simultaneous secular and libration behaviors (Ely et al., 2009).

Phase plots constitute the classical method to study these orbits. They observe the evolution over a lunar sidereal period. Folta et al. 2006 employed this approach and plotted the signatures of short period variations in both the eccentricity and the argument of periapsis. Frozen orbits were also found at different initial conditions. Furthermore, findings show that for every lunar sidereal period of 27.32 days; the motion of the eccentricity versus the argument of periapsis repeats. This evolution also encircles a point on the polar plot, and for a fixed configuration of semi-major axis and inclination, the pattern is independent of the initial values of eccentricity and argument of periapsis as part of the translation theorem. The magnitudes of those elements vary while the shape and evolution remains nearly identical (Beckman et al., 2007). Semrud et al, 2009 investigated polar plots of the evolution of eccentricity and argument of periapsis in order to find a stationary point around these elements revolves.

Another effort to find stable orbits was performed by Ramanan et al., 2005[10]. They studied the impact of inclination on orbital lifetime for low altitude lunar orbits. They propagated a baseline orbit, with an initial altitude of 100 km, at different initial inclinations and at a fixed RAAN. The results presented the existence of various inclination windows that showed instability, at which the orbit lifetime was severely shorter compared to more stable inclination regions. In their analysis, two gravity models provided comparable results: LP100J and LUN60D. According to their model, an inclination of 95 degrees gives a maximum decay in the periapsis altitude of only 26 km in two years, while at 11 degrees, the orbital lifetime reaches its minimum of 16 days. For these unstable orbits, even if the sma remains nearly constant, the drastic change in eccentricity accelerates the decay of the spacecraft [].

Most studies suggest that the main cause of such unstable regions encountered by low altitude orbiters are the mascons in the crust of the celestial body of study. In addition to that, for fast spin bodies such as Mars, orbit stability may be affected by spin-orbit resonance effects. Some publications have studied the implications of spin-orbit resonances, especially on repeating ground tracks for geodetic applications. Repeating ground tracks imply that the satellite passes occur only at particular longitudes, and therefore the effects of the mascons may be enhanced or diminished, depending on the situation. In particular, previous work from He and Huang (2015)[11] analyzed the existing low ‘number' resonances in the Mars case. This, together with the mascon influence in Low Mars Orbits (LMO) may cause severe instabilities for certain orbital element configurations. In the case of Mars, the most recent gravity models, developed with data acquired from the Mars

Reconnaissance Orbiter (MRO) have improved significantly the accuracy of the propagation. Since Mars is becoming a target for upcoming missions, it is fundamental to address the challenges the orbiting satellites face, including a potential correlation between resonance and stability.

Our goal in this paper is to study the stability of low altitude Martian orbits, to determine the effects of the spin-orbit resonance in those orbits, and to identify potential unstable orbital element configurations that should be avoided as part of the mission design. This paper presents a detailed and comprehensive study of the orbital stability of the red planet, including an analysis of the influence of the spin-orbit resonance in the orbit lifetime. The first section places the focus on Mars spin-orbit resonances. We applied known computational methods based on the literature to find theoretical resonances at Mars, to compare them with the results from numerical orbit propagation in the results. The second section focusses on the assumptions used for this analysis, including the applied gravity field in the simulation, the orbital elements range, and the tools and software utilized. In the third section, we present the results of the numerical propagations of a large set of initial orbital element configurations, which are grouped in initial orbit inclinations. In the fourth section, we introduce an introductory analysis of slightly elliptical orbits, which will be an emphasis in future work. Finally, in section five, we draw some conclusions based on the obtained numerical data.

SPIN-ORBIT RESONANCE

Resonance is a common phenomenon in nature. Sometimes resonance can involve destabilizing behavior. For instance, when two bodies have their orbital period correlated by a ratio of two small integers, they are in orbital resonance, the bodies exchange momentum and shift their orbits until the resonance that caused that is no longer present. In some particular cases, a resonant system can correct itself and remain stable, keeping that configuration. We can find resonance in co-orbiting bodies such in the Jovian system or when a spacecraft orbits the Earth and is in resonance with the Moon.

Spin-orbit resonances slightly differ from that idea since the planet rotation is involved. It is also a well-known research topic, especially for Earth orbiting satellites. There are several applications that rely on spin-orbit resonance, such as precise gravity recovery measurements and geodesy (Klokočník et al., 2012)[12]. The resonance is defined as the ratio of two co-prime integers that correspond to the number of passes completed per rotation of a celestial body. According to Wagner, Gooding and Allan[13], a satellite is in orbital resonance with a rotating body when it performs β revolutions, or beta from now on, over α rotations, or alpha. This occurs in the presence of a precessing orbit mainly caused by the zonal harmonic, J_2. The analytical derivation of the spin-orbit resonance effect has been carried out by several previous publications. Reigber, 1989, stipulated that resonance occurs when the derivative of the resonance angle, $\phi_{\beta/\alpha}$, introduced by Gooding and King-Hele, 1989[14], is negligible or singular. Translated in mathematical terms:

$$\dot{\phi}_{\beta/\alpha} = \alpha(\dot{\omega} + n + \dot{\sigma}) + \beta\left(\dot{\Omega} - \dot{\theta}\right) \approx \alpha n - \beta\dot{\theta} \qquad (1)$$

where n is the mean motion, $\dot{\theta}$ is the mean angular rate of rotation of the celestial body, $\dot{\sigma}$ is the time derivative of the traditional M_0 in Kepler's equation, i.e., the mean anomaly at epoch such that $M = \sigma + nt$, and $\dot{\omega}$ and $\dot{\Omega}$ are the secular rates of the argument of periapsis and the Right Ascension of the Ascending Node (RAAN) respectively. The linear variation with time of the orbital elements are known and represented as follows: (Kaula, 1966)[15].

$$\dot{\omega} = -\frac{3}{4} n J_2 \left(\frac{R}{a}\right)^2 (1 - 5\,cos^2 I)(1 - e^2)^{-2}$$

$$\dot{\Omega} = -\frac{3}{2} n J_2 \left(\frac{R}{a}\right)^2 cosI\,(1 - e^2)^{-2}$$

$$\dot{\sigma} = -\frac{3}{4} n J_2 \left(\frac{R}{a}\right)^2 (1 - 3\,cos^2 I)(1 - e^2)^{-2}$$

For nearly circular orbits where we can neglect the terms in e^2, and after applying the condition for resonance we get

$$n = \frac{\beta}{\alpha}\left(\dot{\theta} - \dot{\Omega}\right) - \dot{\omega} - \dot{\sigma}$$

and if we input the preceding rates into the above equation and take n as $\frac{\beta}{\alpha}\dot{\theta}$ we can arrive to Equation 6.

$$n' = \frac{\beta}{\alpha}\dot{\theta} - \frac{3}{4} J_2 n' \left(\frac{R}{a}\right)^2 \left[5\,cos^2 I - 2\frac{\beta}{\alpha} cosI - 1\right]$$

Since we have the mean motion in both sides of the equation, and even a which is also related to it by Kepler's third law, we need to solve this equation iteratively. We followed the same procedure as in Klokočník et al., 2003[16], where they start by considering an initial estimate of in the form of just $n' = \frac{\beta}{\alpha}\dot{\theta}$, and then they perform another iteration to place the previous result for a and n'. This solution is only accurate to first order in J_2, however it is sufficient to find resonant regions of interest that can be further studied by numerical integration simulations, being that the approach we take in this paper.

Klokočník et al, 2003, also pointed out the issue of considering the orbital elements in the equations above as mean elements rather than osculating elements, which are subject to the Lagrange Planetary Equations (LPE). In the resonance context, the choice for utilizing mean elements is of particular importance since each osculating element of the LPE for a particular term of the geopotential can lead to many terms in the integrated result. While most of these terms are short periodic (they vary with M), some other can also be secular. Certain orbits may, for some of the orbital elements, give short periodic terms that yield also long periods, defining the phenomenon of near resonance (Klokočník et al., 2003). In this paper, we compute the resonances based in the intuitive time-averaged semimajor axis or a''. This formulation of the mean semimajor axis was used by Brouwer and differs from other derivations introduced for instance by Kozai, where he introduced the term a_k, where the time averaged value of the residual $\boldsymbol{r} - \bar{\boldsymbol{r}}$ is zero to first order. Our semimajor axis value, a'', is then defined by Equation 7.

$$a'' = a'(1 + \frac{2}{3} J_2 F)$$

Where the quantity F is the product of three factors defined by three main mean elements, a, e and I, as seen in Equation 8.

$$F = \frac{3}{4}\left(\frac{R}{a}\right)^2 (1 - e^2)^{-\frac{3}{2}}\,(2 - 3sin^2 I)$$

The same derivation can be utilized for distinct celestial bodies by applying the right constant terms. For the case of Mars we selected 7.088e-5 rad/s for the rotation rate, and equatorial radius of 3396.2 km, a gravitational parameter of 4.282e13 m/s^2 and 1960.45e-6 for J_2. He and Huang, 2015 also applied this technique to find orbit resonances at Mars, although they used a different iterative method to find relevant semimajor axis values, and they focused on nearly circular nearly polar orbits first and highly elliptical orbits later. Their approach was to investigate the resonance framework at Mars to enable gravity recovery missions, since they stipulated that the absence of resonance implies little contributions to the orbital perturbations by some high degree and order coefficients (He and Huang, 2015).

We applied the method explained above to orbits with different inclinations: 0, 30, 60, and 90 degrees. This procedure helped us to find the right region where the lowest resonances remain in terms of planet rotations, since it is easier to study ground tracks. For those, we placed our focus on the 14:1 and 13:1 cases because they give some of the lowest altitudes for single planet rotation resonances. After doing this, we ran numerical simulations around those regions to study the effects on orbit stability by looking at the results of the propagation. Figure 1 shows the spin-orbit resonance plots for spacecraft in the inclinations of interest and at low semimajor axis values. The horizontal axis in the plot is the number of rotation, or alpha, and the vertical axis in the plot is the time-averaged semimajor axis, *a''*, previously introduced. The numbers to the right of each case correspond to the beta value, or the number of passes, i.e., ground tracks. We will use these values to find resonant orbits around the theoretical time-averaged semimajor axis, *a''*. Since we cannot input the mean sma in our model and only initial values, we would approximate our numerical propagation by introducing an initial sma that is close enough to the values computed analytically. After that we will run large propagation sets of initial conditions above and below the analytical value, with just 1 km step, in order to cover the whole region and to observe the over-resonance and the under-resonance, as well as the transition from the studied resonance to

other higher orders where the effects in stability are not as prominent as in the low resonance regime.

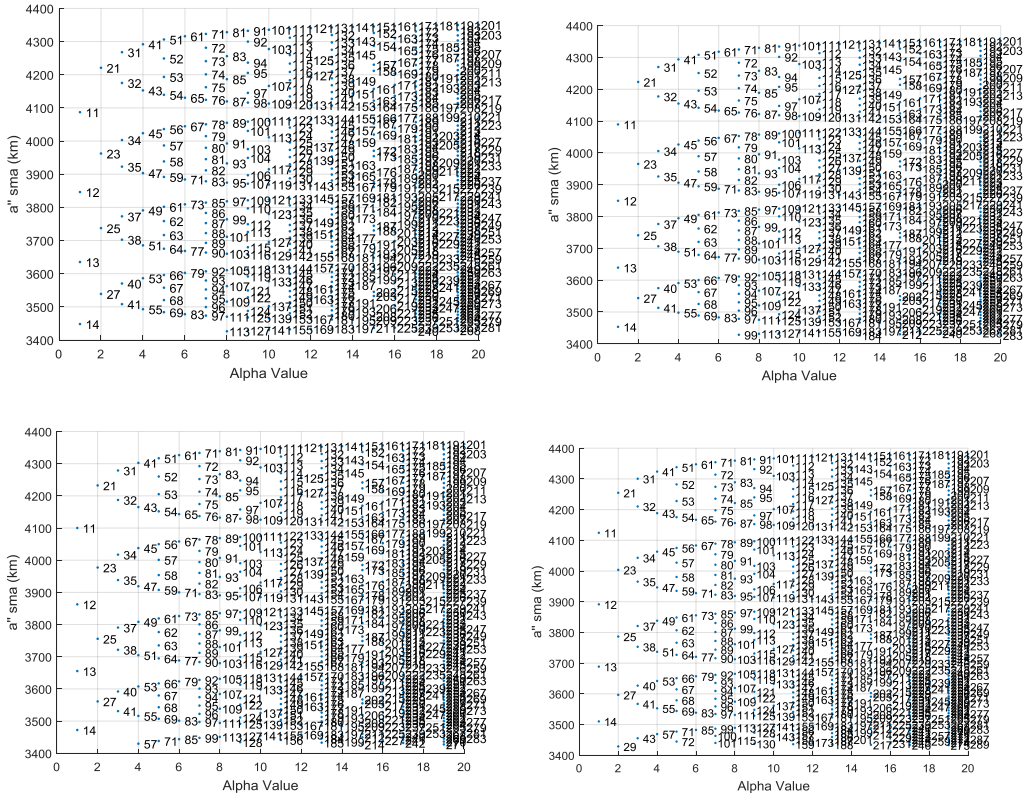

Figure 1: Spin-orbit resonance plots for a circular Mars orbiting satellite. The images represent 0, 30, 60 and 90 deg inclined orbits respectively from top left to bottom right, and for equivalent altitudes from 30 to 1000 km. The mean semimajor axis for each case can be found in the y-axis, the number of rotations, or alpha, in the x-axis, and the number of passes, or beta, next to each data point.

To visualize the effects of a changing inclination for an analytically computed low resonant orbit, we calculated the semimajor axes for the 11:1, 12:1, 13:1, and 14:1 resonances, at all initial inclinations with a 1 deg step. Figure 2 shows the results of this analysis, as well as the case of interest, 14:1 resonance, separately. In this figure, for a 14:1 resonance, the difference in mean semimajor axis from an equatorial to a polar orbit is around 70 km. Therefore, some initial altitudes may have a low resonance for certain inclinations but not for others.

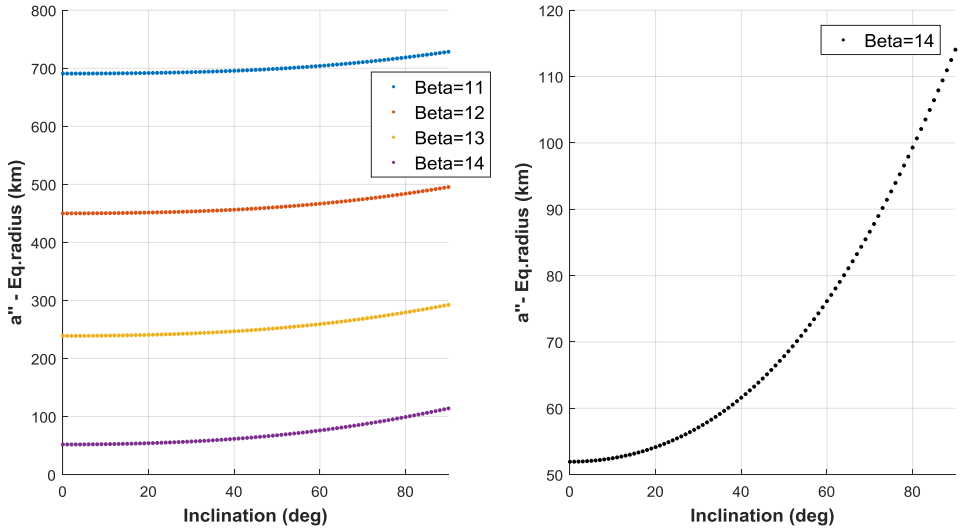

Figure 2: Difference of sma depending on the initial inclination for low rotation spin-orbit resonances with Mars circular orbits. To the left, 11:1, 12:1, 13:1, and 14:1 resonances plotted all together. To the left, the case of interest, 14:1 resonance. The sma difference can be as high as 70 km depending on the chosen inclination.

Our method consists on studying the decay of the orbits around the low resonances of interest to observe any potential correlation between the two phenomena. Some of these low resonances correspond to sma values that are impractical for mission design purposes due to severe atmospheric drag. However they are interesting since the potential effects of the mascons in the decay may be more pronounced and easier to distinguish. Therefore, although we are aware of the impracticality, and due to the choice of an absent atmospheric model in our simulations, we consider them in our analysis.

We group the simulations in subsets categorized by the initial inclination, which at the same time will indicate the semimajor axis values where those resonances exist. Hence, for each selected inclination, the sma values will be different according to Figures 1 and 2. Our main finding is that the mean semimajor axis values that correspond to low spin-orbit resonances imply greater orbit instability than higher order resonances. Therefore, orbits that have that mean semimajor axis are at a higher risk of severe decay. The cause of that effect may have different origins. We theorize that frequent repeating ground tracks over large mascons can cause higher gravity accelerations, perturbed the orbit more significantly leading to a faster and more sensible decay. These mascons would affect the orbit at the beginning tremendously, especially at lower altitudes, such in a way that could lead to a surface impact or ,depending on the ballistic coefficient, make the satellite pass through high drag areas that over time can also imply a crash with the Mars surface. The idea is therefore to run numerical orbit propagations that correspond to low alpha resonances, where only a planet rotation occurs. After that, we store the evolution of the orbital elements and compute the minimum altitude achieved to see how much the orbit was perturbed over a certain time period. Once we identify initial configurations that lead to the worst cases, we check if initial LANs correspond to repeating ground tracks over certain known mascons, according to previous publications regarding the Mars gravity field (Konopliv et al.).

The resonance state is temporary and evolves naturally (Klockonick et al., 2003). A spacecraft in orbit may start at a specific resonance when it gets inserted in the right initial orbit parameters, and then pass through it to another resonance order. The time that takes to happen may depend on how tightly the resonance begins. Another explanation could be an effect of how well aligned the passes may be with large mascons. Especially in the cases where the satellite is passing repeatedly over larger mascons at low altitudes, the orbit may get more perturbed than in cases where the same resonance is achieved, but the satellite avoids them. This means that the orbit will be temporarily in the resonance state that was first inserted into but will morph to other resonance states later since the orbit is being perturbed severely, i.e., eccentricity is growing and AOP is drifting. Therefore, for mission applications with requirements to pass over certain regions repeatedly, orbit maintenance may be needed. In addition, significant altitude drops may also require maneuvers due to severe atmospheric drag acting on the spacecraft. In our simulations we are not considering atmospheric drag, but if the orbit altitude decays to values under 200 km, the effects of atmospheric drag at Mars are stronger and a collision may occur sooner or later, depending on the ballistic coefficient of the spacecraft.

SIMULATIONS AND METHOD

We carried out large sets of numerical orbit propagations. The approach was to take different altitude regimes where the smallest beta/alpha ratios were present, and at different inclinations. We placed our focus in nearly circular orbits at selected inclinations to utilize the equations presented in the previous section, and to not consider the effects of different initial values for the argument of periapsis (AOP).

We chose the MRO110C gravity model (Konopliv et al, 2016), with 70x70 harmonics. Since we are studying only the effects of the gravity field on very low orbits, we have not included any atmospheric model in the integration, nor solar radiation pressure effects. The influence of third body effects from Phobos and Deimos in low altitude orbits is almost negligible for this case, although it was considered in the propagator. The main regions of interest were chosen at four particular inclinations: 0, 30, 60, and 90 degrees. The idea is to study if there is any influence of the latitude of the mascons by running these orbit inclinations. Each simulation set was studied around a mean semimajor axis that corresponds to a low number resonance and a low geodetic altitude (since the orbit are nearly circular), to study potential stability threats or surface impact. For the case of Mars, and for low initial altitudes of 50-1000 km, the lowest existing resonances are 14:1, 13:1, 12:1, and 11:1, when considering only one planet rotation, i.e., alpha equal to one. We focused on only one planet rotation to simplify the analysis, since it is more intuitive to find trends in the location of the passes and the density of the ground tracks in that scenario, especially at the beginning of the propagation.

The simulations used semimajor axis steps of 1 km for a particular region of interest and for each inclination. For all cases, the LAN increments were 5 or 10 deg to cover a reasonable amount of initial longitudes around the planet. The AOP is not defined for circular orbits, so once the perturbations start to act on the satellite and the orbit shape starts to change as the eccentricity grows, the AOP validity starts to appear. We decided to add an almost negligible eccentricity of 0.0001 at the beginning of the propagation to keep an initially defined AOP at 270 deg, i.e., around the South Pole, to maintain a similar scenario and maintain consistency among the studied orbits. Later, we ran preliminary investigations of eccentric orbits that revealed that periapsis located the South Pole represents the most stable configuration, for more information refer to Future work section. For all our simulations we always started at a true anomaly of 0 deg. To compute the LAN, we created a

custom angle, which is independent of the epoch, as opposed to the RAAN parameter. The LAN was defined as the dihedral angle between a line of nodes vector and the X axis vector of the Mars Fixed reference system, about the Z axis vector of the same reference system.

With resonance phenomena as the cause of the repeating ground tracks, the idea is to study the effects of resonance in the overall orbit stability. Typically, as seen in previous lunar orbit stability work, perturbations from irregular gravity fields cause the orbits to morph in shape and have an eccentricity drift that has a periodic nature in the case of stable orbits, or decays to impact in the case of unstable orbits. Therefore, the eccentricity oscillates in amplitude in a particular period of time, unless the propagation is too much altered, leading to impact. We run the simulations for 180 days which is a sufficient time to observe most of the eccentricity oscillation periods, while saving computational time over lengthy durations. For each orbit, we aim to find a characteristic minimum altitude achieved that corresponds to a periodic and local maximum of the eccentricity in the overall orbit. Longer propagations would give similar minimum altitudes achieved due to the periodic behavior, unless the local maximum of the eccentricity, or minimum value of the altitude of periapsis, is still not found, which could happen for some cases. For those, still the minimum value of the altitude presented in our graph would be representative of an extreme case where the altitude drops significantly.

Although not proven yet, the premise is that the satellites, when present in a resonance region, have repeating ground tracks that depending on the initial insertion configuration, may be above regions where the mass concentrations, are more prominent, or the opposite, regions where their absence also causes anomalies in the gravity field. Konopliv et al., studied the different gravity influences depending on the latitude and longitude regions, creating a detailed field map that can be seen in Figure 4. They used 2 years of tracking data collection obtained from the Mars Reconnaisance Orbiter (MRO), which allowed them to improve significantly the global gravity field at Mars. Further work that included the entire MGS radio tracking data, as well as the Mars Odissey orbiter and MRO data was performed to create the MRO110C gravity model in 2012, which we use in this paper.

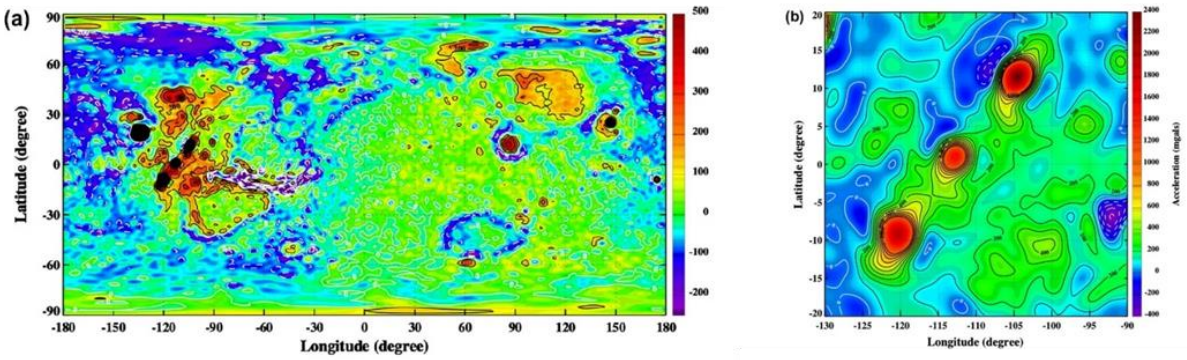

Figure 4: Heatmap for the Mars acceleration. These two plots were originally presented in Konopliv et al., 2010. The plots represent the surface gravity anomalies to degree and order 90 with the MRO110B2 gravity model. Our analysis uses the newer MRO110C and we run propagation at a higher reference altitude. However, these plots help us to identify mascons locations such as Olympus Mons and Tharsis volcanoes Pavonis, Arsia and Ascraeus Mons (bottom image). Valles Marineris presents the minimum acceleration at -658 mGals in this model, which also affects the propagation. Image credits: Konopliv et al., 2010[17].

This heat map show where the largest mascons are located and their influence in the geopotential. The regions around Olympus Mons and Tharsis Montes are especially conflicting since they present some of the highest accelerations. Also, for higher latitudes or inclinations, the near polar region between -150 and -60 deg longitude, as well as the region around the Hellas Planitia, show some negative acceleration that can also affect the orbit stability. An important thing to note is that the conflicting regions, while being mostly below 30 deg latitude, does not directly translate in orbits with equal or lower inclination than that to be very affected. Orbits with even higher inclinations have the capability to go over two or more of this conflicting regions due to the shape of the ground tracks which would be more tilt, in a way that the orbit may even pass over the whole problematic Tharsis region in the same pass, which will be repeated and therefore generating important instabilities.

RESULTS

Initial Survey

We started our simulations with a general set of orbit propagations for different inclinations, to look for potential trends that we could identify in advance. To identify bounding cases, we ran two extremes of inclination: 0, and 90 degrees. For each one we propagated a total of six different initial circular altitudes, ranging from 50 to 200 km in steps of 25 km, and in LAN steps of 30 deg. Our approach is to study the stability by plotting the minimum altitude achieved during the propagation, for which we took a time step of 60 seconds to compute.

By definition, equatorial orbits do not have a defined LAN. However, perturbations and resonant effects are still present and the orbit slightly decays. This is similar to what happens to areostationary orbits, where where J_2 causes a sma oscillation that leads to a periodic motion around a stable point (Colella et al., 2017)[18]. Figure 5 shows a representative low, equatorial orbit where the altitude of periapsis evolution follows a periodic motion, starting at nearly zero eccentricity, i.e., periapsis and apoapsis at almost identical values, and following an uptrend until getting back to zero again.

In contrast, polar orbits showed an interesting behavior, where for certain altitudes, there was a dependency on LAN. One may think the smallest altitudes, in the absence of an atmospheric model in the simulation, would yield the most decay due to their higher proximity to the mascons. However, in our survey, we found the highest decay with respect to the initial altitude at 125 km and not at lower values such as 50 or 100 km. According to the analytical resonance calculations, this would correspond to a region around the 14:1 resonance for that particular inclination, which would explain this behavior and the LAN dependency. Figure 6 shows the typical periodic behavior found in perturbed but stable orbits, as well as the eccentricity growth and extreme orbit reshaping found in unstable orbits. A first look identifies the existence of conflicting initial altitudes (or sma, since we are considering circular orbits) that involves a dependency on the initial LAN, possibly due to the existence of larger mascons at those longitudes.

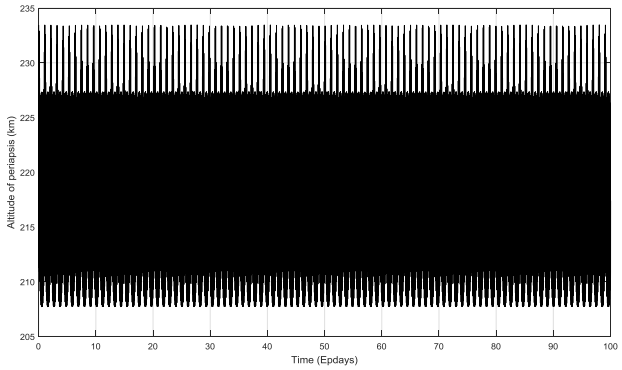

Figure 5: Altitude of periapsis evolution of an initial equatorial circular orbit around the 13:1 resonance region for that inclination. The perturbations act in the satellite causing a small eccentricity variation that makes the satellite entering a periodic oscillation.

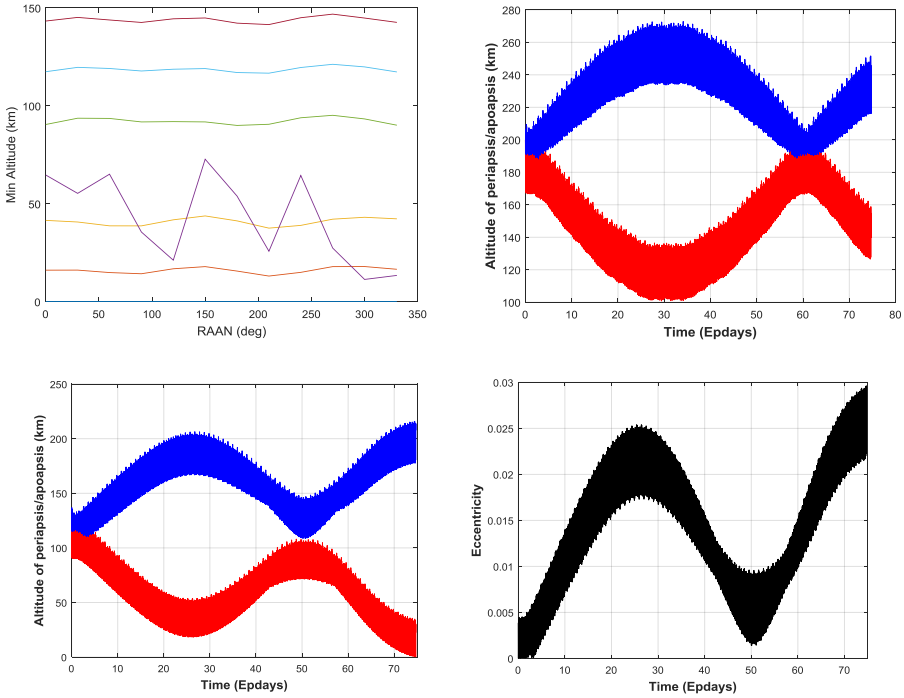

Figure 6: Results of the wide survey for a circular and polar orbit at different initial altitudes or sma. In the upper left plot, we can see how for non-low-resonant orbits, the decay dependency on the LAN is almost negligible, while for a low-resonant orbit, 14:1 in this case, the effects are noticeable. The upper right picture corresponds to the altitude of periapsis/apoapsis evolution of a stable initially 200 km circular orbit at 0 LAN. The bottom left plot shows the case of an unstable for an initially 125 km circular orbit at 300 deg LAN, there we can appreciate the growth in eccentricity that creates the instability and eventual impact, at about 75 days. Lastly in the bottom right, we see the actual eccentricity evolution plot of the former orbit.

Circular Orbit Inclination Studies

After we identified the existence of a potential correlation between the sma values that correspond to low-alpha resonances and a higher decay in general, we proceeded to explore in more detail the trade space by studying the LAN dependency at different inclinations. We carried out simulations by choosing LANs from 0 to 360 deg, with 5 or 10 deg step. We ran those cases for multiple altitude regimes, following always the theoretical resonance altitudes found analytically. We chose the lowest alpha resonance, equal to one rotation, for ease of illustration of the repeating ground tracks. As said before, in all this analysis, the initial AOP is set to 270 deg, which together with a true anomaly of 0 deg, means that we start at periapsis and at the south pole in our nearly circular orbits with 0.0001 eccentricity. Therefore, we need to take into account that the initial altitudes account for the smaller polar radius rather than the traditional equatorial radius of 3396.2 km previously introduced.

We started out at 30 deg inclination, at which some of the ground tracks pass over latitudes of where the most prominent mascons are located, according to Figure 4. We ran initial altitudes ranging from 235 km to 245 km, where a 13:1 resonance is located for circular orbits at 30 deg. Figure 7 shows equivalent results at different scales. The plot on the left shows a larger perspective in which the overall decay is not significant nor extremely dependent on LAN, even at this resonance region, while the picture on the right shows a close up plot of the same data, in which some very minor LAN dependencies are distinguishable.

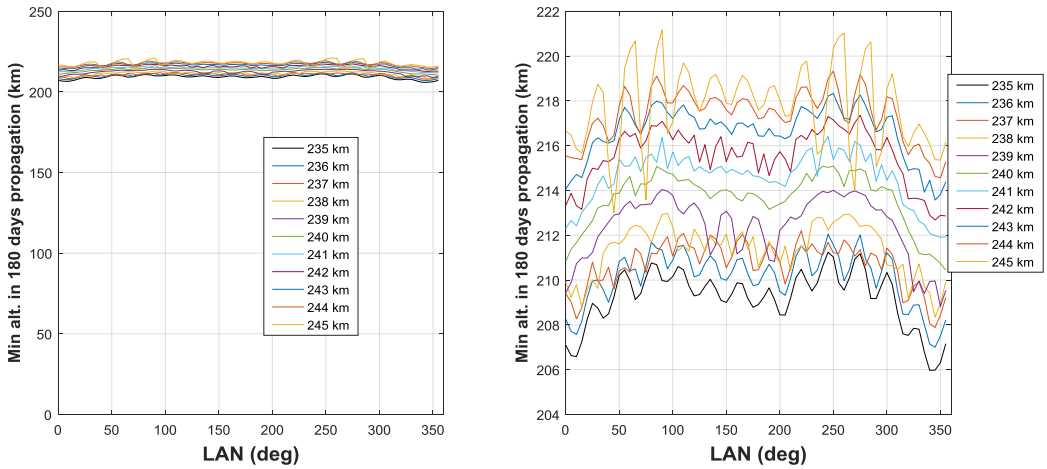

Figure 7: Minimum altitude results of the resonance altitude region around 260 km for nearly circular orbits and 30 degrees of inclination, which corresponds to a 13:1 resonance. On the left side, an overall perspective that shows the results from 0 km to 250 km. On the right side, a close up image to see the LAN dependency.

A potential explanation of not having strong decays is that while some main mascons may be within 30 deg latitude such as Olympus Mons, the orbit inclination implies ground tracks that are not sufficiently tilt to pass right above them or a combination of them. That, combined with a slightly higher altitude, could be the cause of a smaller decay compared to the higher inclination cases. At 60 degrees inclination instead, some high elevation regions such as the Tharsis Montes, composed by the Arsia, Pavonis, and Ascraeus Mons, can be crossed entirely, during the same pass.

According to the analytical calculations, the 14:1 resonance for a 60 deg inclined circular orbit is between 60-80 km altitudes. Figure 8 shows four plots that correspond to 1 km increments of altitude in this range, including cases affected by resonance and others not affected by it. We found

that in the low-alpha-resonance region, the orbits become very chaotic, to a point that it is difficult to distinguish a pattern that can lead to some generally stable LAN values. The sensitivity is so great that just 2 deg LAN difference in the initial insertion may lead to a stable orbit as compared to an impact case. Once we are out of the chaotic region, the orbit behavior seems to be more predictable, the perturbations still act on the satellite propagation but there is no risk of impact (without atmospheric drag), even for orbits that start at lower altitudes, as seen in the first upper plot in Figure 8.

Another interesting point is that the peaks and depths in the plots align themselves due to the existence of repeating ground tracks, since we are dealing with a resonant region of 14:1 where it involves just one rotation. If we divide the spheroid of Mars in 14 different initial LANs that are equivalent, the result would be a 25.71 deg step. For cases sufficiently close but still outside the low-alpha resonance region, some initial LANs give similar or almost identical results in terms of minimum altitude than their counterparts that started the propagation at approximately 25.71 deg away in terms of LAN. These orbits may be placed in a higher order resonance regime, however, some of them may start still with ground tracks spaced similarly to the 14:1 resonance until they complete the higher order beta/alpha ratios. Since the actual resonance is higher, and the ground tracks eventually achieved more coverage after some planet rotations, the shape of the orbit does not get as much perturbed. This scenario can be found in the initially circular 75-80 km region in Figure 8, where we can see a LAN equivalence spaced in 14 distinguishable peaks. Figure 9 shows in two plots the 13:1 resonance region results for a 60 deg nearly circular orbit. In those plots we can corroborate how even at higher altitudes, which are more pertained for actual mission design, the resonance effects in stability are present.

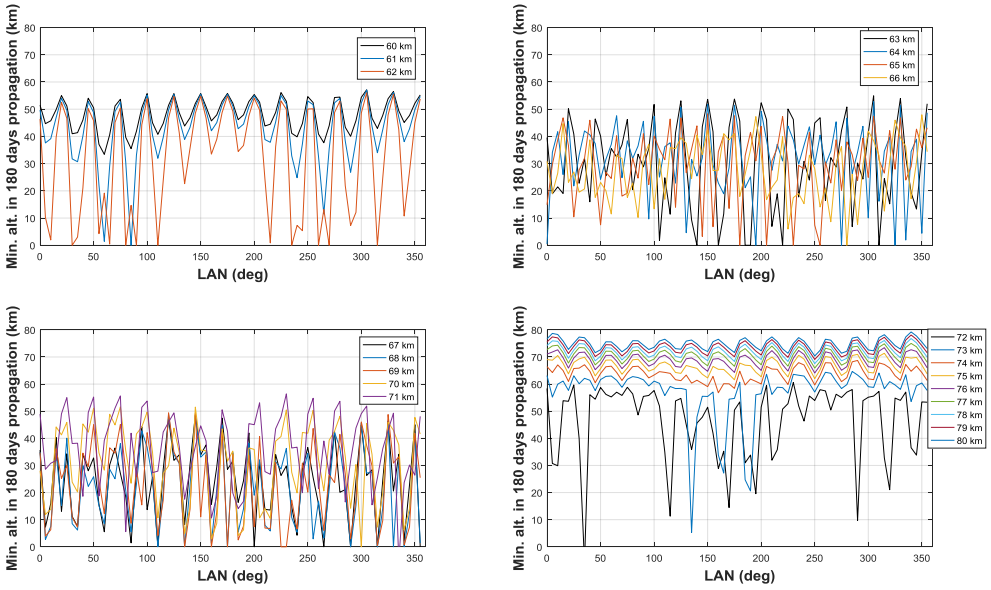

Figure 8: Minimum altitude achieved plots in 180 days for a variety of initial semimajor axis and for an initially 60 deg circular orbit inclination. The plots are distributed in groups to see the chaotic behavior presented at initial sma that correspond to a 14:1 resonance. In some of those cases, for particular LANs, the satellite even crashes. For cases outside the low resonance, orbits are stable for any LAN, even at lower initially circular altitudes such as 60 km, in the upper left.

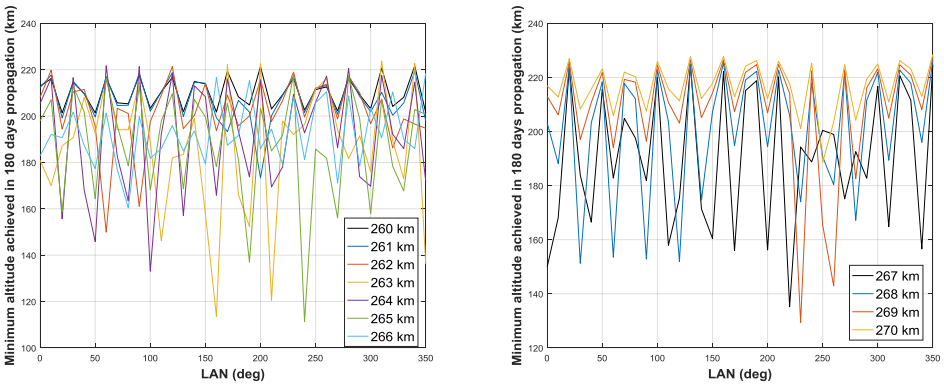

Figure 9: Minimum altitude plots for a region surrounding a 13:1 resonance at 60 deg inclination for a nearly circular orbit. The plots show the higher decay of the initial sma or altitude values when the low-alpha resonance is present as compared to other bounding cases, at 260 or 270 km where the decay is more controlled.

The sensitivity to orbit insertion in the low-alpha resonant states is very high, implying impact or stable orbits for differences in the initial LAN as low as a few degrees. For example, for an initially circular 67 km altitude, and at an initial LAN of 148 deg we get an impact case while just by moving one degree the initial LAN to 147 deg, we get a more sustainable orbit. This could be explained by studying the repeating ground tracks. When the orbit passes very close or right above large mascons, the orbit is more perturbed and quickly loses the initial low resonance state. Therefore, it has that state for several passes until leading to a decay in altitude that in some cases results in an impact. Then it is important to remember that the resonant state is temporary as the orbit gets perturbed and the spacecraft may move to other higher order resonances. The amount of time involved in this process may depend on how much the orbit is perturbed by having the repeating-ground tracks aligned with the mascons or not.

That is possibly the most intuitive explanation. However, when we look at the ground tracks, we can observe, as in Figure 10, that some impact cases do not actually even hit the largest mascons nor they lose significantly the initial low-alpha resonant state. Therefore, a further more detailed study is required to analyze the causes of the relationship between the orbit decay and the low resonance regimes at low altitudes. In this paper, our initial conclusion is that we cannot rely on low resonant orbits without maintenance at these low altitudes since precisions in the order of a few degrees in the LAN insertion are hard to achieve in terms of maneuver and orbit determination accuracies.

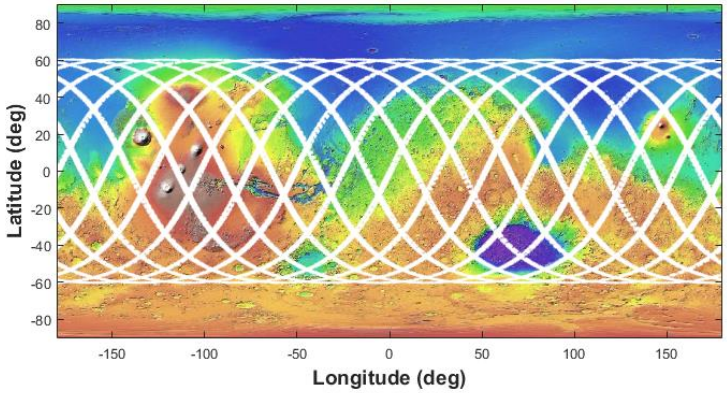

Figure 10: Ground tracks for an initially 3463.2 km semimajor axis, 0.0001 eccentricity, 60 degrees inclination, and 58 deg of LAN. The orbit impacts with the surface after 148 days. The 14:1 resonance is quite preserved during that period of time as seen in the plot. In this case, the repeating ground tracks do not pass significantly above the highest acceleration mascons located at Olympus Mons and Tharsis Montes. They pass over Hellas Planitia instead, which may be a cause for the decay.

Lastly, we placed our focus again in polar orbits. They are of significant interest due to their capability to potentially achieve global coverage. Because of this, resonance is relevant since missions with a global coverage requirement need to avoid repeating ground tracks in the low-alpha resonance regime. At the same time, they are also important since they enable the study of all the mascon regions around the planet. We focused on values around the semimajor axis we found in our initial survey, which for a circular orbit would be an equivalent 125 km altitude, or a 14:1 resonance. Therefore, we ran a subset of cases from 110 to 140 km altitude, all at 90 degrees, to observe the whole region around this low-alpha resonance. Figure 11 shows the results from that analysis where we can distinguish a similar effect, perhaps even more chaotic, compared to the 60 deg inclination case exposed in Figure 8.

When the satellite is located at a sma value that corresponds to the low-alpha resonance, the orbit decay is significantly more unstable than at higher order resonances. For polar orbits, satellites also have the capability to pass over areas with a significant acceleration gradient. In particular, at the north pole, according to the heat map from Figure 4 there are extensive regions with negative acceleration, which may be combined with repeating passes over high positive acceleration mascons, potentially causing a disruption in terms of stability. We chose one particular case to illustrate the ground track behavior over time. Figure 12 shows an initially circular polar orbit at 124 km initial altitude, and the ground track plots at 10, 90, and 141.8 days, at which the case impact the surface of Mars. The orbit corresponds to a 120 deg LAN. The resonance, as commented before, is not perfect unless maintained with correction maneuvers and it drifts after a period of time. Therefore the density of the ground tracks gets reduced and eventually the satellite may move to another resonance state, which would be generally of higher order, allowing the spacecraft to achieve more coverage if the lifetime mission is sufficiently long. In this case, the orbit starts at an accurate 14:1 resonance, with a small drift after 90 days. Eventually, the 14:1 resonant state is practically morphed to a higher order right before the orbit impacts the surface of Mars at 141.8 days.

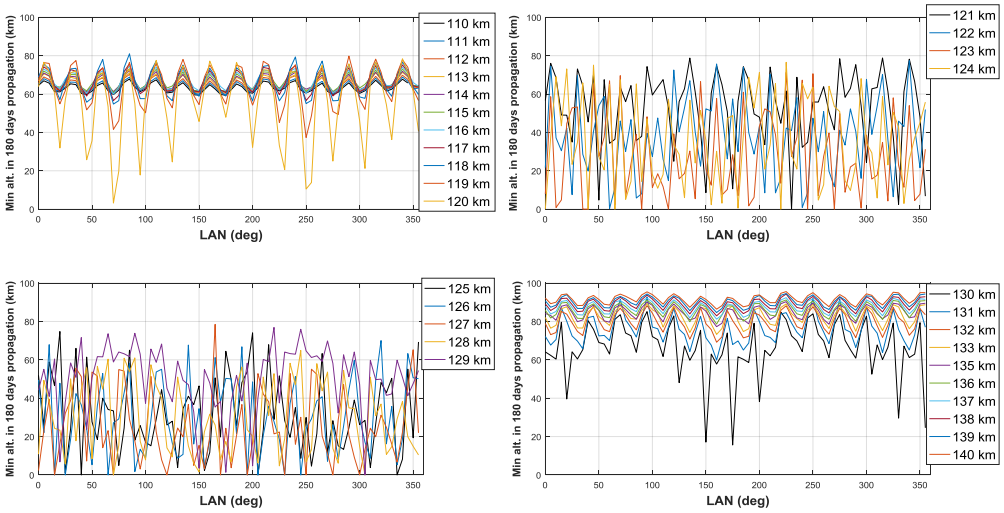

Figure 11: Minimum altitude results for an initially near circular polar orbit for altitudes around a low-alpha resonance of 14:1. In the first plot in the top left, the effects of the low-alpha resonance start to be noticeable at 120 km. The top right and bottom left images show the chaotic environment caused by hitting the 14:1 resonance, leading to great instability which is dependent on the initial LAN. The last image, on the bottom right shows how by inserting a spacecraft outside the low-alpha resonance altitude region, the orbit is stable with a small variance of minimum altitude achieved depending on the initial LAN. AOP was set initially to 270 deg with a nearly circular orbit with 0.0001 eccentricity.

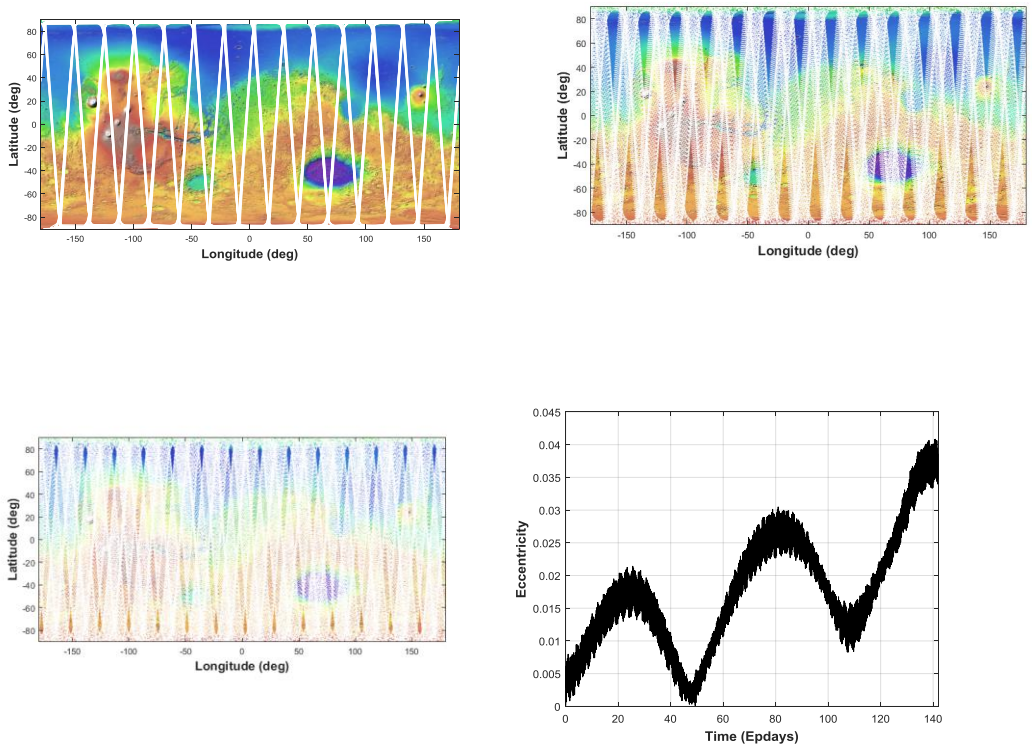

Figure 12: Ground track evolution at 10, 90, and final impact at 141.8 days for an initially nearly circular polar orbit at 124 km. The orbit reshaping is significant as seen in the last bottom right image, making the eccentricity grow in size until achieving a final impact.

ELLIPTICAL ORBITS AND FUTURE WORK

The study of the same correlation between low-alpha resonances and stability for elliptical orbits is very interesting. He et al., 2015 previously studied the analytical spin-orbit resonance formulation of Highly Elliptic Orbits at Mars. Since the orbits have a non-negligible eccentricity, the terms in *e* in Equation 5 cannot be ignored, and the theoretical resonances change. Also, the argument of periapsis adds a new degree of freedom that needs to be further studied. Future work on elliptical orbits is fundamental to know more about the causes of the link between the two phenomena. We present a preliminary analysis in this section of some elliptical orbit cases. For investigations involving argument of periapsis, we use a visual tool that takes into consideration this new dimension. The initial AOP will play a significant role, as the LAN did in the circular orbit simulations.

Figure 13 introduces a graphical approach following the method in Plice & Craychee (2011). The graph represents a conceptual design space covering the range of orientations for the line of nodes and the line of apsides. All combinations of LAN and AOP have the same values of *a*'', *e*, and *i*, respectively 3512 km, 0.005, and 85 degrees for the example in Figure 14. This *a*, *e*, *i* set produces

14:1 resonance for some combinations of LAN and AOP, e.g. 0, 0 degrees, but not for all cases in the grid.

The heat map color codes take the LAN and AOP axis values as the initial conditions and portray the delta in periapsis altitude from the initial state to the minimum value within the specified duration, in this case 80.65 Mars sols. While tightly resonant cases experience significant instability, in line with the reinforcement hypothesis presented earlier, higher order resonances can produce quasi-stable patterns. Non-resonant cases exhibit attributes of frozen orbits and appear in the white band at 270 deg argument of periapsis. The most pronounced orbital decay occurs in cases with the periapsis near the equator.

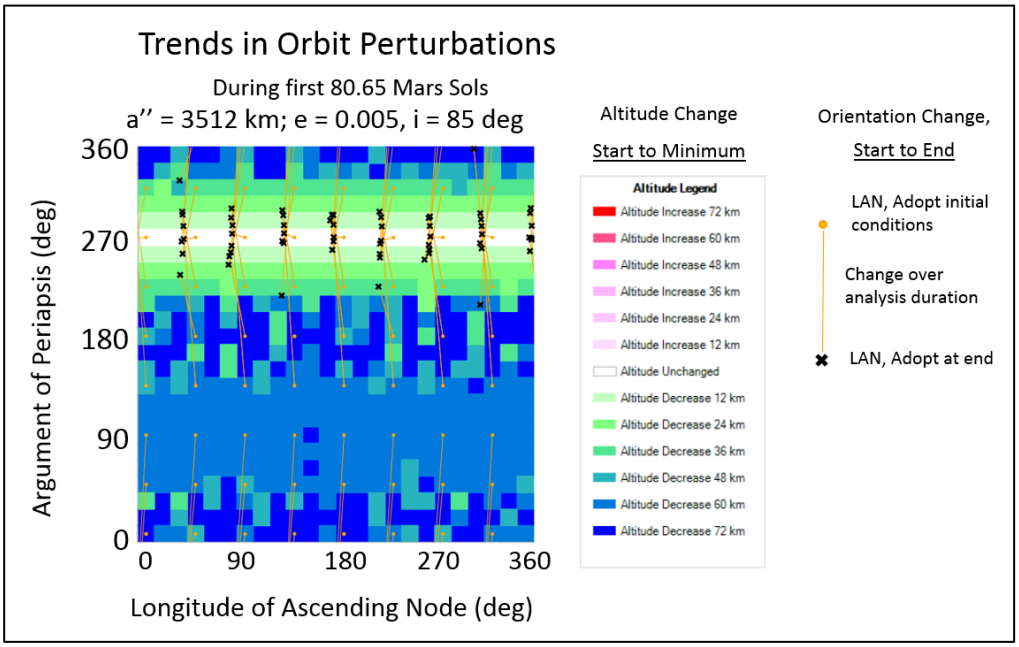

Figure 13: Graphical approach for representing gravitational perturbations in eccentricity and orientation, with repeating cycles of LAN overlaid. The most pronounced decay occurs when the initial conditions orient the periapsis near the equator, while placement of the periapsis near the south pole can exhibit frozen orbit characteristics.

The trend layer overlay on the heatmap depicts the net change in the orientations of the line of nodes and the line of apsides from the initial states to the end of the period of interest. Orange dots show the initial conditions evenly located on an 8 x 8 grid. Each line segment ends with a black "X," positioned according to the final LAN, AoP conditions at the selected stop time. Isolated orange dots represent cases where impact occurred during the selected timespan. With Mars' high rotation rate (compared to Luna) the 80.65 sol time interval allows the value of the LAN parameter to encompass all longitudes many times. When the combined influence of the orbit period and nodal precession produces repeated ground tracks over the planet surface, the orange line segments take vertical slope (not shown), however not all members of the grid exhibit resonance and the x-dimension offset in endpoint can identify non-resonant cases. Figure 15 captures the convergence of all cases in the example toward placement of the periapsis near Mars' south pole, thus portraying the apsidal precession effect of gravitational perturbations.

While the orbits under study have altitudes too low for practical mission applications, further research may reveal similar patterns associated with higher altitude alpha=1 resonance. In this initial investigation, we focus on three comparison cases, all with initial LAN value of 0 degrees:

initial AoP values of 0, 90, and 270 degrees. Figure 15 shows the dramatic differences in altitude outcomes from positioning the initial periapsis in the three example positions. The previous figure used just over 80 Mars sols to depict complete altitude decay in the AoP = 0 deg case, near-minimum altitude value in the AoP = 90 deg case, stability in the AoP = 270 deg case, and the ground track repetition pattern.

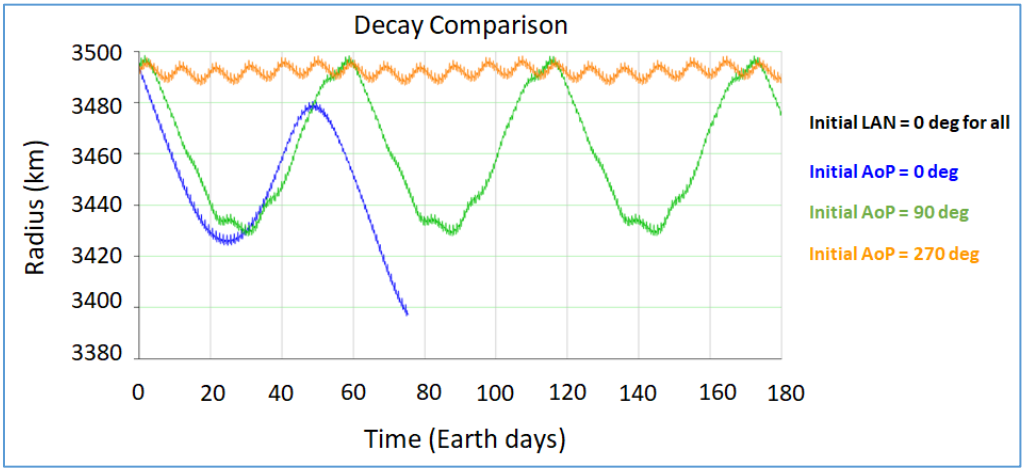

Figure 14: Altitude history comparison of three LAN, AoP initial condition pairs: decay to impact at 0, 0 deg, quasi-stable behavior at 0, 90 deg, and frozen orbit at 0, 270 deg.

At LAN and AoP initial values of 0 deg, the orbit begins with a resonant pattern and decays to impact relatively quickly. At initial LAN of 0 deg with initial AoP at 90 deg, the orbit shows periodic cycles that persist for at least one Earth year. We believe this to be an example of higher order resonance influences. At initial LAN of 0 deg and initial AoP of 270 deg, the orbit displays frozen altitude and orientation for at least one Earth year. Figure XX illustrates 180 Earth days of the three cases representing different regimes of perturbed motion.

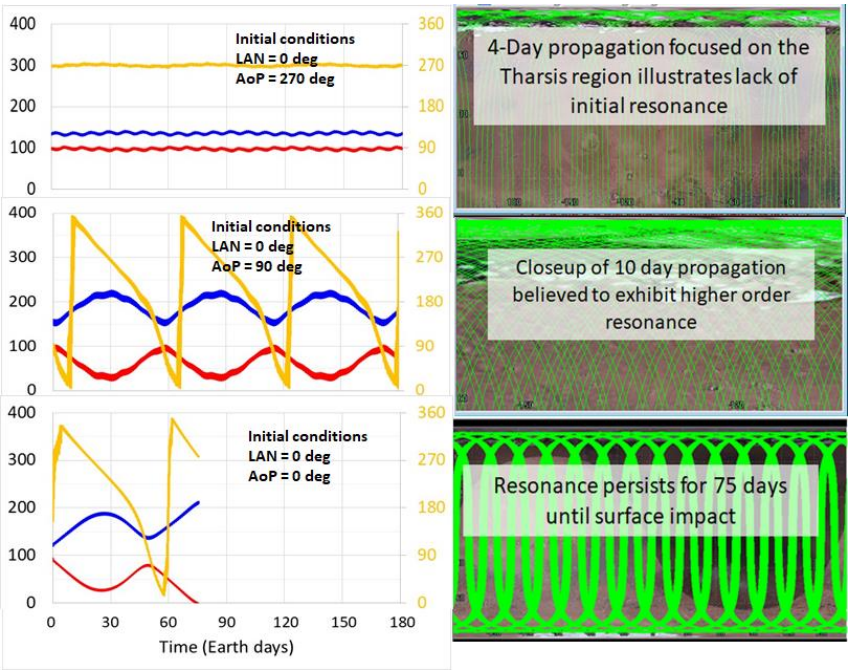

Figure 15: Further comparison of three LAN, AoP initial condition pairs showing frozen orbit stability with non-repeating ground tracks, quasi-stable cyclic patterns believed to associate with high alpha resonance, and severe instability in correlation with re.

CONCLUSION

We studied the stability effects that spin-orbit resonances create in low altitude orbits. We started out by applying the resonance theory to the Mars environment to create beta/alpha, i.e., passes per rotation, plots according to a set of initial inclinations and semimajor axes. Those maps helped us to identify initial orbit sizes where low resonant orbits were present. We chose these regions since their easy identification helps us to study in more detail the outcome of a satellite in these orbits, by analyzing a manageable number of repeating ground tracks that can be observed to see if there are mascons that are directly perturbing the orbit stability severe by changing its shape.

For convenience, we focused our efforts in the 14:1 and 13:1 resonances since correspond to the lowest altitudes with only one planet rotation for all the inclinations of interest. After identifying those starting altitudes through mathematical formulation, we ran the regions that were around that particular resonance to study the behavior at different starting LANs. Our unit of measurement was to look at the minimum altitude achieved in 180 days, to see if by choosing different LANs, the effects were different due to the existence of known mascons in Mars, especially in regions such as Olympus Mons or Tharsis.

We found that for relevant inclinations that allow the ground tracks to pass well above those regions, the orbit is severely perturbed, in some cases leading to a collision. Due to the chaotic environment, the LAN study didn't give safe or unsafe regions for stable orbits since the sensitivity is too high and in some cases differences of just a deg in LAN at the moment of insertion can become critical. Especially at 60 and 90 deg inclination, the ground tracks allow the spacecraft to cover repeatedly regions with a significantly higher acceleration than the rest of the planet, as found in previous Mars gravitational studies. If the orbit starts out in a low resonance that ensures several initial passes on those regions, the orbit is quickly perturbed, modifying its shape, jumping to other resonances and even crashing in some cases. If the initial LAN ensures that the satellite does not

pass over those problematic regions, the orbit may maintain the low resonance for a while until smaller mascons slowly also alter it, but it may become stable for a while.

ACKNOWLEDGMENTS

The authors would like to thank the support from the NASA Ames Research Center management, in particular from Ryan Vaughan, chief of the Mission Design Division. Also, we would like to acknowledge the contribution of Ronald L. Evans for creating a custom tool to visualize the heat maps exposed in the future work section. As always, enduring gratitude goes to the late Professor Harm Buning, whose many students of orbital mechanics included Mercury, Gemini, and Apollo astronauts.

REFERENCES

Klokocnik, J., Bezdek, A., Kostelecky, J., & Sebera, J. 2010, Journal of Guidance, Control, and Dynamics, **33** 853

Klokočník, J., Kosteleckỳ, J., & Gooding, R. 2003, Journal of Geodesy, **77** 30

Kaula, W. M. 1966, Theory of Satellite Geodesy. Applications of Satellites to Geodesy (London: Blaisdell, Pub. Co.)

S. Konopliv, Alex & Park, Ryan & M. Folkner, William. (2016). An improved JPL Mars Gravity Field and Orientation from Mars Orbiter and Lander Tracking Data. Icarus. 274. 10.1016/j.icarus.2016.02.052.

Silva, Juan & Romero, P. (2013). Optimal longitudes determination for the station keeping of areostationary satellites. Planetary and Space Science. 87. 14–18. 10.1016/j.pss.2012.11.013.

Alvarellos, Jose. (2009). Technical Note: Perturbations on a Stationary Satellite by the Longitude-Dependent Terms in Mars' Gravitational Field. The Journal of the Astronautical Sciences. 57.

M. Górski, Krzysztof & Bills, Bruce & S. Konopliv, Alexander. (2018). A high resolution Mars surface gravity grid. Planetary and Space Science. 160. 10.1016/j.pss.2018.03.015.

Konopliv, A., S. W. Asmar, E. Carranza and W. L. Sjogren, D. N. Yuan, "Recent Gravity Models As a Result of the Lunar Prospector Mission," *Icarus*, Vol. 150, No. 1, 2001, pp. 1-18.

Folta, D. and D. Quinn, "Lunar Frozen Orbits," AIAA 2006-6749, AIAA/AAS Astrodynamics Specialist Conference and Exhibit, Keystone, CO, 21-24 August, 2006.

Plice, L., K. Galal, & J. Burns (2017). "DARE Mission Design: Low RFI Observations from a Low-altitude, Frozen Lunar Orbit." AAS 17-333, 2017 AAS/AIAA Space Flight Mechanics Meeting, San Antonio, TX, Feb. 5 – 9, 2017.

Zuber M., Smith D., Watkins M., Asmar S., Konopliv A., Lemoine F., Melosh J., Neumann G., Phillips R., Solomon S., Wieczorek M., Williams J., Goossens S., Kruizinga G., Mazarico E., Park R., Yuan D. 'Gravity Field of the Moon from the Gravity recovery and Interior laboratory (GRAIL) Mission'. Science, Vol 339. 8th February 2013.

Ely T., Lieb E. 'Constellations of Elliptical inclined lunar orbits providing polar and global coverage'. AAS 05-343.

K. W. Meyer, J. J. Buglia and P. N. Desai, "Lifetimes of Lunar Satellite Orbits," NASA Technical Paper 3394, March 1994.

R. V. Ramanan and V. Adimurthy, "An Analysis of near Circular Lunar Mapping Orbits," *Journal of Earth System Science*, Vol. 114, No. 6, 2005, pp. 619-626.

P. M. Muller and W. L Sjogren, “Mascons: Lunar Mass Concentrations,” *Science*, Vol. 161, No. 3482, 1968, pp. 680-684.

A. Konopliv, S. W. Asmar, E. Carranza and W. L. Sjogren, D. N. Yuan, “Recent Gravity Models As a Result of the Lunar Prospector Mission,” *Icarus*, Vol. 150, No. 1, 2001, pp. 1-18.

Gupta S., Sharma R. K. “Effect of Altitude, Right Ascension of Ascending Node and Inclination on Lifetime of Circular Lunar Orbits”. International Journal of Astronomy and Astrophysics, 2011, 1, 155-163.

R.B. Roncoli. “Lunar Constants and Models Document”. Jet Propulsion Laboratory, 2005.

A. Abad, A. Elipe and E. Tresaco, “Analytical Model to Find Frozen Orbits for a Lunar Orbiter,” *Journal of Guidance, Control, and Dynamics*, Vol. 32, No. 3, 2009, pp. 888-898.

On fine orbit selection for particular geodetic and oceanographic missions involving passage through resonances

Sensitivity study of high eccentricity orbits for Mars gravity recovery

Zhi-Zhou He[1,2] and Cheng-Li Huang[1]

2015 National Astronomical Observatories of Chinese Academy of Sciences and IOP Publishing Ltd.
Research in Astronomy and Astrophysics, Volume 15, Number 1

An improved JPL Mars gravity field and orientation from Mars orbiter and lander tracking data

Alex S. Konopliv ∗,RyanS. Park ,WilliamM. Folkner

Klokocnik, J., Gooding R. H., Wagner C. A., Kostelecky J., Bezdez A. The Use of Resonant Orbits in Satellite Geodesy: A Review
Surv Geophys
DOI 10.1007/s10712-012-9200-4

Received: 11 March 2011 / Accepted: 28 June 2012

Coverage of Mars by Probes Slightly Off the Areostationary Orbit

Elena Colella [1] • Emiliano Ortore [1] • Christian Circi [1] • Ennio Condoleo [1]

Received: 12 September 2016 / Accepted: 3 March 2017 / Published online: 18 March 2017

Earth Moon Planets (2017) 120:31–39
DOI 10.1007/s11038-017-9504-y

…HERE. AFTER ALL ITEMS HAVE BEEN COPIED TO THE FORMATTED LIST BELOW THIS POINT

REFERENCES

Konopliv, A., S. W. Asmar, E. Carranza and W. L. Sjogren, D. N. Yuan, "Recent Gravity Models As a Result of the Lunar Prospector Mission," *Icarus*, Vol. 150, No. 1, 2001, pp. 1-18.

Folta, D. and D. Quinn, "Lunar Frozen Orbits," AIAA 2006-6749, AIAA/AAS Astrodynamics Specialist Con-ference and Exhibit, Keystone, CO, 21-24 August, 2006.

Plice, L., K. Galal, & J. Burns (2017). "DARE Mission Design: Low RFI Observations from a Low-altitude, Frozen Lunar Orbit." AAS 17-333, 2017 AAS/AIAA Space Flight Mechanics Meeting, San Antonio, TX, Feb. 5 – 9, 2017.

Alvarellos, Jose. (2009). Technical Note: Perturbations on a Stationary Satellite by the Longitude-Dependent Terms in Mars' Gravitational Field. The Journal of the Astronautical Sciences. 57.

M. Górski, Krzysztof & Bills, Bruce & S. Konopliv, Alexander. (2018). A high resolution Mars surface gravity grid. Planetary and Space Science. 160. 10.1016/j.pss.2018.03.015.

S. Konopliv, Alex & Park, Ryan & M. Folkner, William. (2016). An improved JPL Mars Gravity Field and Orientation from Mars Orbiter and Lander Tracking Data. Icarus. 274. 10.1016/j.icarus.2016.02.052.

Konopliv, A., S. W. Asmar, E. Carranza and W. L. Sjogren, D. N. Yuan, "Recent Gravity Models As a Result of the Lunar Prospector Mission," *Icarus*, Vol. 150, No. 1, 2001, pp. 1-18.

Folta, D. and D. Quinn, "Lunar Frozen Orbits," AIAA 2006-6749, AIAA/AAS Astrodynamics Specialist Con-ference and Exhibit, Keystone, CO, 21-24 August, 2006.

Plice, L., K. Galal, & J. Burns (2017). "DARE Mission Design: Low RFI Observations from a Low-altitude, Frozen Lunar Orbit." AAS 17-333, 2017 AAS/AIAA Space Flight Mechanics Meeting, San Antonio, TX, Feb. 5 – 9, 2017.

[5] Silva reference goes here

[6] Meyer, K. W., J. J. Buglia and P. N. Desai, "Lifetimes of Lunar Satellite Orbits," NASA Technical Paper 3394, March 1994.

[7] Abad, A., A. Elipe and E. Tresaco, "Analytical Model to Find Frozen Orbits for a Lunar Orbiter," *Journal of Guidance, Control, and Dynamics*, Vol. 32, No. 3, 2009, pp. 888-898.

[8] Lara reference goes here

[9] I found a citation with Ely as the sole author but not "et al."

[10] Ramanan et al.

[11] Zhi-Zhou and Chengli

[12] Klokocnik et al., 2012

[13] Wagner, Gooding and Allan

[14] Gooding and King-Hele, 1989

[15] Kaula, 1966

[16] Klockcnik et al., 2003

[17] Konopliv et al., 2010

[18] Colella et al., 2017